



**HAL**  
open science

# Distributed Source Seeking via a Circular Formation of Agents Under Communication Constraints

Lara Briñon Arranz, Luca Schenato, Alexandre Seuret

► **To cite this version:**

Lara Briñon Arranz, Luca Schenato, Alexandre Seuret. Distributed Source Seeking via a Circular Formation of Agents Under Communication Constraints. *IEEE Transactions on Control of Network Systems*, 2015, 3 (2), pp. 104 - 115. 10.1109/TCNS.2015.2428391 . hal-01358978

**HAL Id: hal-01358978**

**<https://hal.science/hal-01358978>**

Submitted on 2 Sep 2016

**HAL** is a multi-disciplinary open access archive for the deposit and dissemination of scientific research documents, whether they are published or not. The documents may come from teaching and research institutions in France or abroad, or from public or private research centers.

L'archive ouverte pluridisciplinaire **HAL**, est destinée au dépôt et à la diffusion de documents scientifiques de niveau recherche, publiés ou non, émanant des établissements d'enseignement et de recherche français ou étrangers, des laboratoires publics ou privés.

# Distributed Source Seeking via a Circular Formation of Agents under Communication Constraints

Lara Briñón-Arranz, Luca Schenato, *Member, IEEE*, and Alexandre Seuret

**Abstract**—This paper addresses the source seeking problem in which a group of autonomous vehicles must locate and follow the source of some signal based on measurements of the signal strength at different positions. Based on the observation that the gradient of the signal strength can be approximated by a circular formation of agents via a simple weighted average of the signal measured by each agent, we propose a combination of a cooperative control law to stabilize the agents to a circular formation and a distributed consensus-based source seeking algorithm, which is guaranteed to steer the circular formation towards the vicinity of the source location. In particular, the proposed algorithm is provided with two tunable parameters that allow for a tradeoff between speed of convergence, noise filtering and formation stability. The benefit of using consensus-based algorithms resides in a more realist discrete time control of the agents and in asynchronous communication resilient to delays, which is particularly relevant for underwater applications. The analytic results are complemented with numerical simulations.

**Index Terms**—Distributed control, multi-agent systems, source seeking, consensus algorithms, lossy communication

## I. INTRODUCTION

Detecting the source of a signal is relevant to many complex applications such as environmental monitoring [23], search and rescue operations [14], odor source detection [19], sound source localization [34] and pollution sensing [17]. Source localization is also a fundamental problem in nature. Inspired by the behavior of some bacteria, which are able to find chemical sources, the problem of seeking a maximum using autonomous vehicles is studied in [18], [21].

There are various approaches to deal with this topic in the current literature. For example, several source seeking algorithms are based on gradient-descent methods. If it is available, the gradient of the signal strength can be used to produce a gradient-descent algorithm for a vehicle or group of vehicles [2]. However, in practice, the agents are only capable of measuring the signal strength and the gradient information is usually unknown. In this situation, the gradient can be approximated using spatially distributed measurements of the signal distribution. In the literature there are two different strategies to collect distributed measurements. The first one uses a single vehicle that changes its position over time in order to measure the signal propagation at different locations [1], [2], [3]. The other option consists in multiple

vehicles collaborating to collect concentration measurements at multiple locations [23], [22].

The application of extremum-seeking techniques to the source localization problem has been analyzed under different constraints using a single nonholonomic vehicle [33], [8]. The idea is to add an excitatory input to the vehicle steering control in order to approximate the gradient of the signal strength and to use this information to drive the vehicle towards the source. Novel stochastic approaches based on the classical extremum-seeking algorithm are introduced in [1], [18], [26]. A recent paper [20] proposes a strategy to steer a single integrator robot to the maximum of a scalar field without explicit gradient estimation. The main disadvantage of both strategies is that in order to collect sufficient information, the vehicle may have to travel large distances, delaying the vehicle's convergence to the source. The authors of [13] extend the classical idea of extremum seeking into a discrete-time multi-agent scenario showing improved convergence and robustness.

Collaborative methods using multi-agent systems have been proposed in recent literature. In [9], [23] a group of vehicles equipped with appropriate sensors estimates the model parameters of the scalar field via collected measurements. A least-squares approximation is applied in order to steer the group of agents to the source location. Other works are based on distributed estimation of the concentration plume [24], [25]. In this case, the function signal is estimated or approximated and the source localization becomes a distributed optimization problem. The authors of [7], [11] propose different least-squares estimation algorithms to locate peaks of a scalar field generated by a network of radial basis Gaussian functions. These strategies rely on a prior model of the signal distribution, which might not be known a priori if the environment is unknown.

Other approaches to cooperative estimate the gradient of the signal are available. For example, a collaborative control law to steer a circular formation of nonholonomic vehicles to the source of a signal distribution using only their direct signal measurements is presented in [22]. Following the same idea, the authors of [36] present a centralized algorithm based on leader-follower strategies in which the gradient is estimated by using a least-squares method. In [15] a distributed source seeking algorithm is proposed using optimization techniques. A source seeking algorithm based on consensus filters is presented in [16] to deal with limited communication. The main drawback of these works is that the spatial propagation of the signal is assumed to be quadratic or concave. Motivated by behaviors of fish groups seeking darker regions, the authors of [28] proposed a distributed source seeking algorithm for a group of vehicles with no explicit gradient estimation.

This work was supported by the EU FP7 Network of Excellence project HYCON2 and the ANR project LimCoS contract number 12 BS03 005 01.

L. Briñón-Arranz is with the CNRS, LAAS, 7 avenue du Colonel Roche, F-31400 Toulouse, France (e-mail: lbrinona@laas.fr).

L. Schenato is with the Department of Information Engineering, University of Padova, Via Gradenigo 6/a, Padova, Italy (e-mail: schenato@dei.unipadova.it).

A. Seuret is with the CNRS, LAAS, 7 avenue du Colonel Roche and Univ. de Toulouse, LAAS, F-31400 Toulouse, France (e-mail: aseuret@laas.fr).

Another interesting approach is presented in [35] and [29] for the 2- and 3-dimensional cases respectively. In both papers, a Kalman filter is used to estimate the value of the scalar field of interest, its gradient and Hessian at the center of a formation of double-integrator agents. The shape of the platform formation is defined in order to minimize the error in the estimates and a cooperative formation control law is designed to asymptotically achieve the optimal formation shape. Based on the same formation control, and using a  $H_\infty$  filter to estimate the value and gradient of the field at the center of the formation, the authors of [30] propose a switching strategy to choose between individual and cooperative search for a group of simple integrator robots to deal with the source seeking task. These works propose a decoupled strategy to solve both cooperative motion and filtering problems for mobile sensor platforms using simple dynamics for the vehicles. However, the communication constraints between the agents are not considered.

The present paper addresses an alternative solution to the source localization problem. In order to locate the source of a scalar field, we consider a group of vehicles equipped with sensors that measure the field of interest such as temperature, salinity, or pollutant flow. In this situation, the fleet of vehicles can be seen as a mobile sensor network. We exploit preliminary results from [4], [5] in which a group of vehicles, uniformly distributed in a circular formation, is able to estimate the gradient of the measured signal. No prior knowledge of the environment or convexity of the signal field is required. The problem is tackled in a 2-dimensional space, hence the configuration considered is a planar formation. Using a cooperative control law from our previous work [6], a group of vehicles modeled with non-holonomic dynamics can be stabilized to a circular formation that tracks a time-varying center. In order to maintain the formation and to steer its center towards the source location, we propose a distributed algorithm based on the multidimensional Newton-Raphson consensus strategy from [32]. The suggested strategy thus inherits the desirable properties of consensus algorithms [10], namely their simplicity, their potential implementation with asynchronous communication schemes, their ability to adapt to time-varying network topologies, and their resilience to packet loss and random delay.

The rest of the paper is organized as follows. First, Section II presents the problem statement including the model of the agents, the cooperative motion control strategy to achieve a time-varying circular formation and some assumptions on the signal strength. Section III provides preliminary results on gradient estimation and additional analysis. Section IV exposes the main contribution, a distributed consensus-based source seeking algorithm. The performance of the proposed strategy is analyzed through numerical simulations in Section V. Finally, we present our conclusions and future directions.

## II. PROBLEM FORMULATION

The main objective of this paper is to design a distributed algorithm to steer a group of agents to the source location of a field of interest. The problem is divided to two steps. Firstly,

the agents, modeled with nonlinear dynamics, are stabilized to a desired particular formation. Secondly, a distributed algorithm allows the agents to estimate the gradient of the scalar field at the center of the formation and drives the center towards the source location using the estimated gradient. For the sake of simplicity, we focus on the 2-dimensional case.

### A. Agents

Consider a group of  $N$  identical vehicles modeled with unicycle kinematics subject to a simple non-holonomic constraint such that the dynamics of agent  $i = 1, \dots, N$  are defined by

$$\begin{aligned} \dot{r}_i &= v_i [\cos \theta_i \ \sin \theta_i]^T \\ \dot{\theta}_i &= u_i, \end{aligned} \quad (1)$$

where  $r_i \in \mathbb{R}^2$  is the position vector of agent  $i$ ,  $\theta_i$  its heading angle and  $v_i, u_i$  are the control inputs. We assume that each vehicle knows its absolute vector position  $r_i$  with respect to the inertial frame.

The first objective of this paper is to stabilize the multi-agent system (1) to a uniformly distributed circular formation. A circular formation of agents is considered in this paper for two main reasons. As will be shown in next section, the measurements collected by a group of sensors uniformly distributed in a circle allow the estimation of the gradient of a signal strength at the center of the circle. On the other hand, some underwater and aerial vehicles are not able to stop at the source position due to physical constraints (e.g., if the linear velocity cannot be zero, see [27]).

We want to design a feedback control to ensure the convergence of the agents to a circular motion with given radius  $D > 0$ , angular velocity  $\omega_0 \neq 0$  and time-varying center  $c(t) = [c_x \ c_y]^T \in \mathbb{R}^2$ . In a practical situation, the given center may be an external reference corrupted by noise or may not be available to all the agents, thus, we assume that each agent supplies its own reference center  $c_i \in \mathbb{R}^2$ . Thanks to the circular control law presented in Theorem 1 from our previous paper [6], each agent modeled by (1) converges independently to a circular motion around its center  $c_i(t)$ . In order to compute this circular control law, the first and second derivatives of  $c_i(t)$  are needed. If all the agents compute the same center, i.e.,  $c_i = c, \forall i$ , the cooperative circular control law presented in Corollary 1 from our previous work [6] makes the multi-agent system (1) converge to a uniformly distributed time-varying circular formation. In order to achieve the uniform distribution along the circle the agents uses only relative information, specifically, they exchange their heading angles.

Consider now the multi-agent system (1) stabilized to a planar uniform distributed circular formation described by a radius  $D$ , a rotation angle  $\phi_0(t) = \omega_0 t$  and the given center point  $c$ . The position of each agent expressed in discrete time at instant  $k$  is given by the following equation:

$$r_i(k) = c(k) + DR(\phi_i)e = c(k) + e_i(k) \quad (2)$$

where  $\phi_i = \phi_0(k) + i\frac{2\pi}{N}$  is the rotation angle,  $R(\phi) = \begin{bmatrix} \cos \phi & -\sin \phi \\ \sin \phi & \cos \phi \end{bmatrix}$  denotes the rotation matrix and  $e = [1, 0]^T$ .

The communication topology of the agents is defined by means of a graph  $\mathcal{G}$ . Let  $\mathcal{G} = (V, E)$  be an undirected communication graph. The set of nodes (agents) is denoted by  $V = \{1, \dots, N\}$  and the set of edges  $(i, j) \in E$  represents the communication links. Let  $P \in \mathbb{R}^{N \times N}$  denote a doubly stochastic matrix, i.e., a matrix whose elements are non-negative,  $P\mathbf{1} = \mathbf{1}$  and  $\mathbf{1}^T = \mathbf{1}^T P$ , where  $\mathbf{1} := [1, \dots, 1]^T \in \mathbb{R}^N$ .  $P$  is consistent with a graph  $\mathcal{G}$  if  $P_{ij} > 0$  only if  $(i, j) \in E$ . Such matrix  $P$  is also often referred as a *consensus matrix*. The essential spectral radius of a stochastic matrix is defined as  $\text{esr}(P) = \max_{\lambda_i \neq 1} |\lambda_i(P)|$ , where  $\lambda_i(P)$  indicates the eigenvalues of  $P$ . In the sequel,  $\otimes$  denotes the Kronecker product and the bold variables are used to represent vectors containing multi-agent information, i.e.,  $\mathbf{c} = [c_1^T, c_2^T, \dots, c_N^T]^T \in \mathbb{R}^{2N}$  is the vector of all the centers  $c_i, i = 1, \dots, N$ .

According to [6], with a view to uniformly distribute the agents along the circular formation, the communication graph must be at least circulant, such as if each agent communicates only with its close left and right neighbors. It is also proven that, if a distance-dependent communication topology is considered, i.e., each vehicle can only communicate in a certain region delimited by a critical communication radius, then due to the geometric properties of the circle the resulting communication graph is a ring and the corresponding consensus matrix  $P$  is circulant. The distributed approach from [6] ensures that the uniform distribution of the vehicles around the circle is robust to a single agent failure.

### B. Signal strength

Each agent represents a mobile sensor or a vehicle equipped with a sensor that is able to measure the signal strength emitted by the source. In mathematical terms, the signal distribution emitted by the source is a bidimensional spatial function representing the scalar field with a maximum or minimum in the position where the source is located. The distribution of the signal strength in the environment is described by an unknown positive spatial mapping  $\sigma(z) : \mathbb{R}^2 \rightarrow \mathbb{R}^+$ , so that agent  $i$  measures the signal strength at its position  $r_i(k)$  as  $\sigma(r_i(k))$ . We assume here that the signal is emitted by a single source such that the source located at  $z^*$  is the only maximum of the scalar field. Let  $\nabla\sigma(z) = [\nabla_x\sigma(z) \nabla_y\sigma(z)]^T \in \mathbb{R}^2$  denote the gradient vector at  $z$  and  $H_\sigma(z)$  the corresponding Hessian matrix. Therefore, the following assumption is considered.

**Assumption 1** *The function  $\sigma : \mathbb{R}^2 \rightarrow \mathbb{R}$  belongs to  $\mathcal{C}^3$ , i.e., it is continuous up to the third partial derivative,  $\nabla\sigma(z^*) = 0$ ,  $\nabla\sigma(z) \neq 0, \forall z \in \mathbb{R}^2 \setminus \{z^*\}$  and  $H_\sigma(z^*)$  is negative definite. Moreover  $\sigma(z)$  is Lipschitz and there exist positive constants  $a_1, a_2, a_3$  such that  $a_1\|z\|^2 \leq \sigma(z^*) - \sigma(z) \leq a_2\|z\|^2$  and  $\|\nabla\sigma(z)\| \leq a_3\|z\|$ .*

Assumption 1 allows a large class of functions to represent the signal strength of the scalar field of interest. In this paper we also analyze the particular case of quadratic signals. It is well known that there are several physical quantities that satisfy the inverse-square law. In that situation, the intensity of linear waves radiating from a point source is inversely proportional to the square of the distance from the source.

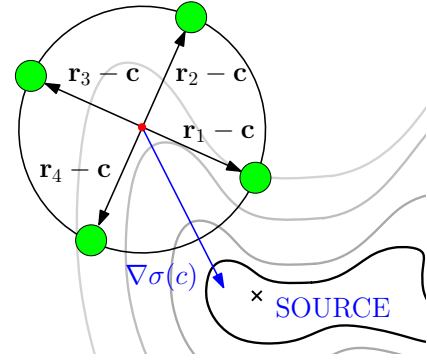


Fig. 1: Collaborative source seeking strategy: the measurements collected by a circular formation of agents are used to estimate the gradient of a signal strength.

For instance, the effects of electrical and magnetic fields as well as light, radiation and sound signals follow an inverse-square law. In a 2-dimensional plane, the signal distributions representing these quantities have quadratic level curves.

Considering a mapping of the inverse of the intensity radiated from a point source, then we obtain a signal proportional to the square of the distance to the source, i.e., a quadratic function. Different mappings could be considered to approximate several scalar fields to quadratic functions. For example, using the natural logarithm (inverse function of the exponential function), a Gaussian distribution can be transformed to a quadratic signal. Therefore, the analysis of quadratic functions is convenient to deal with signal strengths representing sound intensity, irradiance or electromagnetic fields.

### C. Control objectives

Using a gradient-descent algorithm, the group of agents can be driven to the source of the signal distribution, see [2], [22]. Nevertheless, the gradient information is not usually available. In that situation, we propose a cooperative approach in order to satisfy the following control objectives:

- (i) Stabilizing and keeping a circular formation of agents
- (ii) Estimating the gradient
- (iii) Steering the formation towards the source location.

The main purpose of the source seeking is to accomplish objective (iii). The approach proposed in this paper is based on gradient-descent methods and consequently (ii) is required. As it will be presented in Section III, a circular formation is considered to estimate the gradient of the signal and thus the formation control of the agents is an additional objective. In order to accomplish objective (i), we consider a cooperative control law from [6] to stabilize each agent defined by (1) to a circular motion tracking a time-varying center  $c_i$ . In order to keep the formation, the agents must reach an agreement on the centers' positions, therefore a consensus algorithm on centers  $c_i$  is implemented.

The gradient direction of the signal distribution is estimated via concentration measurements collected by the circular formation of agents in Section III. The estimated direction of the gradient will be the reference velocity of the formation

center in order to steer the group of agents to the source location, as represented in Fig. 1. To accomplish the main objective (iii), the common center of the circular formation will be driven towards the source using the estimated direction of the gradient. In order to achieve all of the control aims, we propose the combination of a circular control law from [6] and a distributed algorithm based on the Newton-Raphson consensus method for distributed optimization from [32].

### III. GRADIENT APPROXIMATION

This section presents mathematical results dealing with the gradient approximation of a signal, studying both the general and the quadratic cases.

#### A. Gradient approximation by a fixed circular formation

Consider a circular formation of agents given by (2) taking measurements of a signal distribution  $\sigma(z)$ . Let  $\nabla\sigma(c)$  denote the gradient of  $\sigma(z)$  at the center of the circular formation. Based on the previous result from [5], the following lemma is proposed:

**Lemma 1** *Let  $\sigma : \mathbb{R}^2 \rightarrow \mathbb{R}$  be a bounded function and  $\sigma(r_i)$  be the measure collected by agent  $i$ , where  $r_i$  is the position vector given by (2). Considering a fleet of  $N > 2$  agents uniformly distributed along the circle centered at  $c$  with radius  $D$ , the following equation holds:*

$$\frac{2}{D^2N} \sum_{i=1}^N \sigma(r_i) (r_i - c) = \nabla\sigma(c) + \varphi(D, c) \quad (3)$$

where the approximation error term  $\varphi(D, c)$  satisfies

$$\|\varphi(D, c)\| \leq \lambda_{\max}(H_\sigma)D.$$

*Proof:* Using the first-order Taylor expansion of each measurement  $\sigma(r_i)$  about the point  $c$  and recalling that  $\|r_i - c\| = D$ , then the following equation holds for all  $i = 1, \dots, N$ :

$$\sigma(r_i) - \sigma(c) = \nabla\sigma(c)^T (r_i - c) + \varphi_i(D, c), \quad (4)$$

where  $\varphi_i(D, c)$  denotes the remainder of the Taylor expansion. Multiplying the previous equation by  $\frac{2}{D^2N}(r_i - c)$  and summing over  $i = 1, \dots, N$ , we get

$$\begin{aligned} \frac{2}{ND^2} \sum_{i=1}^N \sigma(r_i) (r_i - c) - \sigma(c) \frac{2}{ND^2} \sum_{i=1}^N (r_i - c) &= \\ \frac{2}{D^2N} \sum_{i=1}^N \nabla\sigma(c)^T (r_i - c) (r_i - c) + \frac{2}{ND^2} \sum_{i=1}^N \varphi_i(D, c) (r_i - c). \end{aligned}$$

Since the agents are uniformly distributed along a fixed circle, then we have  $\sum_{i=1}^N (r_i - c) = 0$  and thus

$$\frac{2}{ND^2} \sum_{i=1}^N \sigma(r_i) (r_i - c) = \frac{2}{ND^2} \left( \sum_{i=1}^N (r_i - c) (r_i - c)^T \right) \nabla\sigma(c) + \varphi(D, c),$$

where  $\varphi(D, c) = \frac{2}{ND^2} \sum_{i=1}^N \varphi_i(D, c) (r_i - c)$ . We analyze the second term of the previous equation using (2) to express the position of the agents  $r_i(k)$  at each instant  $k$  to obtain

$$\begin{aligned} \sum_{i=1}^N (r_i - c) (r_i - c)^T &= D^2 \sum_{i=1}^N R(\phi_i) e e^T R(\phi_i)^T \\ &= D^2 R(\phi_0) \left( \sum_{i=1}^N R(i2\pi/N) e e^T R(i2\pi/N)^T \right) R(\phi_0)^T \\ &= D^2 R(\phi_0) \left( \sum_{i=1}^N \begin{bmatrix} \cos^2(i2\pi/N) & 0.5 \sin(i4\pi/N) \\ 0.5 \sin(i4\pi/N) & \sin^2(i2\pi/N) \end{bmatrix} \right) R(\phi_0)^T \\ &= D^2 R(\phi_0) \left( \frac{N}{2} I_2 \right) R(\phi_0)^T = \frac{ND^2}{2} I_2 \end{aligned}$$

since  $\cos^2 \phi = 1/2(1 + \cos(2\phi))$ ,  $\sin^2 \phi = 1/2(1 - \cos(2\phi))$ , and  $\sum_{i=1}^N \cos(2i\frac{2\pi}{N}) = \sum_{i=1}^N \sin(2i\frac{2\pi}{N}) = 0$  for  $N > 2$ , where  $I_2 \in \mathbb{R}^{2 \times 2}$  represents the identity matrix. Thus, the equality of Eq. (3) is satisfied.

Thanks to the Taylor's Theorem cite each remainder  $\varphi_i(D, c)$  satisfies the inequality

$$|\varphi_i(D, c)| \leq \frac{1}{2} \lambda_{\max}(H_\sigma) \|r_i - c\|^2 = \frac{1}{2} \lambda_{\max}(H_\sigma) D^2, \quad \forall i.$$

Therefore, the function  $\varphi(D, c)$  can be bounded as

$$\|\varphi(D, c)\| \leq \frac{2}{D^2N} \sum_{i=1}^N |\varphi_i(D, c)| \|r_i - c\| \leq \lambda_{\max}(H_\sigma) D.$$

This result provides the gradient estimation of the signal strength at the center  $c(k)$  of a circular formation at each instant  $k$ .

#### B. Gradient computation of a quadratic signal

In this paper we present a new result dealing with the gradient computation in the case of quadratic functions. Following the same ideas of previous Lemma 1, it is shown that the gradient of a quadratic signal can be exactly computed using the measurements collected by a uniform distributed circular formation of sensors. This new contribution is presented in the following corollary.

**Corollary 1** *Let  $\sigma : \mathbb{R}^2 \rightarrow \mathbb{R}$  be a quadratic function such that  $\sigma(z) = z^T S z + b^T z + a$  where  $S \in \mathbb{R}^{2 \times 2}$  is a positive semi-definite matrix,  $b \in \mathbb{R}^2$  and  $a \in \mathbb{R}$ . Let  $\sigma(r_i)$  be the measurement collected by agent  $i$ , where  $r_i$  is the position vector given by (2). Considering a fleet of  $N > 2$  agents uniformly distributed along the circle centered at  $c$  and radius  $D$ , the following equation is satisfied:*

$$\frac{2}{ND^2} \sum_{i=1}^N \sigma(r_i) (r_i - c) = \nabla\sigma(c). \quad (5)$$

*Proof:* Follow the same steps as in the proof of Lemma 1. In the case of quadratic functions and according to the Taylor expansion of  $\sigma(r_i)$  about the point  $c$ , the reminder  $\varphi_i(D, c)$  satisfies

$$\varphi_i(D, c) = \frac{1}{2} (r_i - c)^T H_\sigma(c) (r_i - c) = \frac{1}{2} (r_i - c)^T S (r_i - c).$$

Consequently, the error term of equation (3) becomes

$$\varphi(D, c) = \frac{1}{ND^2} \sum_{i=1}^N (r_i - c)^T S (r_i - c) (r_i - c).$$

According to Eq. (2) representing a circular formation of agents, replace  $r_i$  by (2) to obtain

$$\begin{aligned} \varphi(D, c) &= \frac{1}{ND^2} \sum_{i=1}^N [D^2 e^T R(\phi_i)^T S R(\phi_i) e] (r_i - c) \\ &= \frac{1}{N} \sum_{i=1}^N [R(\phi_i) e e^T R(\phi_i)^T S^T] D R(\phi_i) e, \end{aligned}$$

which can be rewritten as

$$\frac{D}{N} \sum_{i=1}^N \begin{bmatrix} S_{11} \cos^3 \phi_i + 2S_{12} \cos^2 \phi_i \sin \phi_i + S_{22} \cos \phi_i \sin^2 \phi_i \\ S_{11} \cos^2 \phi_i \sin \phi_i + 2S_{12} \cos \phi_i \sin^2 \phi_i + S_{22} \sin^3 \phi_i \end{bmatrix}. \quad (6)$$

Using trigonometric properties, the following equations hold:

$$\begin{aligned}\cos^2 \phi \sin \phi &= (1 - \sin^2 \phi) \sin \phi = \sin \phi - \sin^3 \phi \\ \sin^2 \phi \cos \phi &= (1 - \cos^2 \phi) \cos \phi = \cos \phi - \cos^3 \phi.\end{aligned}$$

The solution of the first term in (6) is reduced by computing  $\sum_{i=1}^N \cos^3(i\frac{2\pi}{N})$  and  $\sum_{i=1}^N \sin^3(i\frac{2\pi}{N})$ . Applying trigonometric properties we obtain  $\cos^3 \phi_i = \frac{3}{4} \cos \phi_i + \frac{1}{4} \cos 3\phi_i$  and then  $\sum_{i=1}^N \cos^3(i\frac{2\pi}{N}) = 0$ . (The same equation holds for  $\sin^3 \phi_i$ ). Therefore, the error term  $\varphi(D, c) = 0$  in the case of quadratic functions and, consequently, equation (5) holds. ■

This result provides an exact computation of the gradient of a quadratic signal  $\sigma(z) = z^T S z + b^T z + a$  at the center  $c(k)$  of a circular formation at each instant  $k$ . The results presented in the previous lemma and corollary are based on the Taylor's Theorem and, although it is beyond the scope of this paper they can be extended to the 3-dimensional case by choosing an appropriate formation in 3D.

### C. Noise analysis

Consider that each vehicle is able to measure the signal strength at its own position by  $\sigma(r_i)$  but the measurements are corrupted by white zero-mean Gaussian noise  $\omega_i \sim \mathcal{N}(0, \sigma_\omega^2)$ . We analyze how the noise affects the gradient approximation presented in Lemma 1. Due to the noised measurements, the previous computed average of weighted relative position vectors from Lemma 1 becomes

$$\frac{2}{ND^2} \sum_{i=1}^N (\sigma(r_i) + \omega_i) (r_i - c) = \nabla \sigma(c) + \varphi(D, c) + \frac{2}{ND^2} \sum_{i=1}^N \omega_i (r_i - c).$$

In order to analyze the influence of noise, the expectation and variance of the last term are studied

$$\mathbb{E} \left[ \frac{2}{ND^2} \sum_{i=1}^N \omega_i (r_i - c) \right] = \frac{2}{ND^2} \sum_{i=1}^N \mathbb{E}[\omega_i] (r_i - c) = 0.$$

Using the same trigonometric properties as in the proof of Lemma 1, the variance  $\text{Var} \left( \frac{2}{ND^2} \sum_{i=1}^N \omega_i (r_i - c) \right)$  can be expressed as

$$\begin{aligned}\mathbb{E} \left[ \frac{4}{N^2 D^4} \sum_{i=1}^N \omega_i^2 (r_i - c)(r_i - c)^T \right] \\ = \frac{4}{N^2 D^4} \sum_{i=1}^N \mathbb{E}[\omega_i^2] (r_i - c)(r_i - c)^T \\ = \frac{4}{N^2 D^4} \sum_{i=1}^N \sigma_\omega^2 (r_i - c)(r_i - c)^T = \frac{2}{ND^2} \sigma_\omega^2.\end{aligned}$$

The variance is inversely proportional to the radius squared, thus, the greater the radius the smaller the influence of noise in the gradient approximation. However, as proven in Lemma 1 the error in the gradient approximation vanishes when the radius tends to zero. Consequently, we conclude that the radius has an important role in the gradient estimation and the noise attenuation.

## IV. DISTRIBUTED SOURCE SEEKING

As presented in the previous section, if the gradient is not available, the direction of the gradient of a signal strength can be approximated by a group of agents distributed uniformly around a circular formation. If we assume all-to-all and instantaneous communication, all of the agents compute the same estimated gradient direction and then this direction can be used to drive the formation towards the source following

---

### Algorithm 1 Distributed source seeking algorithm

---

```

1: for  $i = 1, \dots, N$  do
2:    $h_i(0) = \tilde{g}_i(0) = \tilde{g}_i(-1) = c_i(0) + \sigma(r_i(0))(r_i(0) - c_i(0))$ 
3: end for
4: for  $k = 1, 2, \dots$  do
5:   for  $i = 1, \dots, N$  do
6:      $g_i(k) = c_i(k) + \frac{2}{D^2} \sigma(r_i(k))(r_i(k) - c_i(k))$ 
7:      $\tilde{g}_i(k) = (1 - \alpha) \tilde{g}_i(k-1) + \alpha g_i(k)$ 
8:      $h_i(k) = h_i(k-1) + \tilde{g}_i(k-1) - \tilde{g}_i(k-2)$ 
9:   end for
10:   $\mathbf{h}(k) = (P \otimes I_2) \tilde{\mathbf{h}}(k)$ 
11:  for  $i = 1, \dots, N$  do
12:     $c_i(k) = (1 - \varepsilon) c_i(k-1) + \varepsilon h_i(k)$ 
13:  end for
14: end for

```

---

a gradient-descent method as shown in [5], [22]. However, the all-to-all communication assumption is not realistic and in several situations each agent communicates only with their neighbors.

Our main contribution is to develop a consensus-based algorithm in order to use the collaborative estimation of the gradient direction presented in Lemma 1 and thus, to achieve the source seeking task in a distributed way. The proposed algorithm will provide the trajectory of each center  $c_i$  needed to compute the circular formation control for the multi-agent system (1), in order to drive the formation to the source location. At each instant  $k$ , each agent computes its position  $r_i(k)$ , its center  $c_i(k)$  and its estimated gradient vector  $f_i(k) = \frac{2}{D^2} \sigma(r_i) (r_i(k) - c_i(k))$ . The objective for the agents is now to reach an agreement on the centers' position  $c_i$  and to compute the vector  $f(k)$  at each time  $k$  defined by:

$$\tilde{f}(k) = \frac{1}{N} \sum_{i=1}^N \frac{2}{D^2} \sigma(r_i) (r_i(k) - c_i(k)). \quad (7)$$

According to Lemma 1, (7) is a good approximation of the gradient direction of the measured signal distribution. The aim for the formation is to reach the source location, such that  $\lim_{k \rightarrow \infty} c_i(k) = z^*, \forall i$ .

The proposed source seeking strategy is described in Algorithm 1, which is based on distributed optimization methods presented in [31], [32]. This algorithm presents two main contributions with respect to previous works. The first difference is that the gradient of the signal is unknown; it is estimated by  $\frac{2}{D^2} \sigma(r_i) (r_i - c_i)$  in line 6. Moreover, Algorithm 1 includes local low-pass filtering of the signal  $g_i(k)$  in order to make the algorithm more robust to measurement noise. The low-pass filter is regulated by the parameter  $\alpha$ , which tradeoffs smoothing the signal ( $\alpha \approx 0$ ) with responsiveness to changes of the signal  $g_i(k)$  ( $\alpha \approx 1$ ).

Algorithm 1 works as follows. Lines 6 and 8 are computations used to track the local quantities which are needed to compute the approximate gradient as in Lemma 1. Line 7 is a low-pass filter in which  $\alpha$  regulates the contribution of previous local measurements. Line 10 performs the consensus operation, where  $\mathbf{h} = [h_1^T, \dots, h_N^T]^T$  denotes the column vector

of all the estimates. Operations in line 12 are again local convex combinations of the past and new estimates. This algorithm has two tunable parameters, namely  $\varepsilon$  and  $\alpha$ , which can be used to tradeoff the rate of convergence, robustness to noisy measurements and formation stability. A formal statement of the properties of Algorithm 1 is given in the following theorem.

**Theorem 1** *Let  $\sigma : \mathbb{R}^2 \rightarrow \mathbb{R}$  be a bounded function that satisfies Assumption 1 and  $\sigma(r_i)$  be the measurement collected by agent  $i$ , whose position  $r_i(k)$  is given by (2) after substituting  $c$  with  $c_i$ . Consider Algorithm 1, where  $\alpha \in (0, 1]$ , and  $P$  is a doubly stochastic matrix with essential spectral radius  $\text{esr}(P) < 1$ . Then, there exist  $\bar{\varepsilon} > 0, \bar{D} > 0, \text{ and } \rho > 0$  (possibly depending on  $\alpha$  and on  $\text{esr}(P)$ ) such that, for all  $D \in (0, \bar{D}), \varepsilon \in (0, \bar{\varepsilon})$  and  $c_i(0)$  satisfying  $\|c_i(0)\| < \rho$ , we have*

$$\lim_{k \rightarrow \infty} \|c_i(k) - z^*\| < \gamma(D), \quad \forall i.$$

Therefore, all the centers  $c_i(k)$  converge to the vicinity of the source location  $z^*$ .

*Proof:* See Appendix. ■

Since proof of Theorem 1 is particularly involved, we prefer to give the intuition behind the proof of the theorem and refer the interested reader to the Appendix. The main idea lies on multi-time-scales approaches for standard singular perturbation model analysis [12], which studies the system behaviour by considering the slow and fast dynamics separately.

*Fast dynamics:* If we set  $\varepsilon = 0$ , then  $c_i(k) = c_i(0) = c_i$  for all  $k \geq 0$  and thus, according to Eq. (2) the position of agent  $i$  becomes  $r_i(k) = c_i + DR(\phi_i)e = r_i(0) = r_i$  for all  $k \geq 0$ . This implies that  $g_i(k) = c_i + \frac{2}{D^2} \sigma(r_i)(r_i - c_i)$  for all  $k \geq 1$  and thus  $\forall \alpha \in (0, 1] \tilde{g}_i(k) = c_i + \frac{2}{D^2} \sigma(r_i)(r_i - c_i)$  for all  $k \geq 1$ . Therefore  $\tilde{h}_i(1) = c_i + \frac{2}{D^2} \sigma(r_i)(r_i - c_i)$  and  $\tilde{h}_i(k) = h_i(k-1)$  for  $k > 1$ . As a further consequence, the dynamics of  $\mathbf{h}$  become  $\mathbf{h}(k) = (P \otimes I_2)\mathbf{h}(k-1)$  for  $k \geq 1$ , which implies that

$$\lim_{k \rightarrow \infty} h_i(k) = \frac{1}{N} \sum_{i=1}^N \left( c_i + \frac{2}{D^2} \sigma_i(r_i)(r_i - c_i) \right) = \bar{h}(\mathbf{c})$$

exponentially fast with rate given by  $\text{esr}(P)$ .

*Slow dynamics:* If we insert the steady state of the fast dynamics  $h_i(k) = \bar{h}(\mathbf{c})$  into the slow dynamics we get

$$c_i(k) = (1 - \varepsilon)c_i(k-1) + \varepsilon \bar{h}(\mathbf{c}(k-1)).$$

Since each system is driven by the same forcing term  $\bar{h}(\mathbf{c}(k-1))$ , then  $\lim_{k \rightarrow \infty} c_i(k) - c_j(k) = 0$ , which implies that the circular formation of agents is maintained and their position vectors depend on the common center, such that  $r_i(\mathbf{c})$ . Therefore, we can restrict our attention to the scenario where  $c_i(k) = \bar{c}(k), \forall i$ , which implies that  $\bar{h}(\mathbf{c}(k)) = \bar{c}(k) + \frac{2}{ND^2} \sum_{i=1}^N \sigma(r_i(\bar{c}(k)))(r_i(\bar{c}(k)) - \bar{c}(k))$ . In that situation, each agent computes the estimate of the gradient direction  $\bar{f}(\bar{c}) = \frac{2}{ND^2} \sum_{i=1}^N \sigma(r_i)(r_i - \bar{c})$ . Thanks to Lemma 1 dealing with the approximation via a circular formation of agents of the gradient of a signal strength at the center of the circle, the following equation holds:

$$\bar{h}(\mathbf{c}(k)) = \bar{c}(k) + \bar{f}(\bar{c}(k)) = \bar{c}(k) + \nabla \sigma(\bar{c}) + \varphi(D, \bar{c}).$$

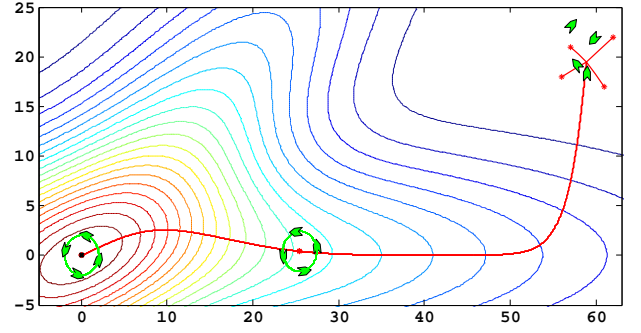


Fig. 2: Four agents implementing a source seeking strategy that is the combination of Algorithm 1 and the circular formation control from [6] ( $\varepsilon = 0.5, \alpha = 1$ ).

And thus the dynamics of  $\bar{c}$  are given by

$$\begin{aligned} \bar{c}(k+1) &= (1 - \varepsilon)\bar{c}(k) + \varepsilon(\bar{c}(k) + \nabla \sigma(\bar{c}) + \varphi(D, \bar{c})) \\ &= \bar{c}(k) + \varepsilon(\nabla \sigma(\bar{c}) + \varphi(D, \bar{c})), \end{aligned}$$

which can be seen as the discretized dynamics with sampling period  $\varepsilon$  of the system

$$\dot{\bar{c}}(t) = \nabla \sigma(\bar{c}(t)) + \varphi(D, \bar{c}). \quad (8)$$

Eq. (8) is a perturbed version of a standard continuous-time gradient ascent, which converges to an equilibrium point under mild conditions. If  $\varepsilon$  is sufficiently small, then the separation of time-scale holds and  $\lim_{k \rightarrow \infty} c_i(k) = \lim_{k \rightarrow \infty} \bar{c}(k)$  converges to a point in the neighborhood of  $z^*$ .

**Remark 1** *Although in the theorem we considered a constant consensus matrix  $P$ , the same conclusion applies even for time-varying consensus matrices  $P(k)$  with possibly random but bounded time-delay, as long as the slow dynamics is sufficiently slow as compared to the convergence rate of the product of the consensus matrices  $P(k)$ , as presented in [31]. Since the slow dynamics are regulated by the tunable parameter  $\varepsilon$ , this requirement is always fulfilled. Thus, asynchronous communication does not impair the algorithm, however  $P(k)$  still needs to be doubly stochastic in order to compute the exact average of the local vectors  $\tilde{h}_i(k)$ .*

Algorithm 1 generates the trajectories of the centers  $c_i$  to drive a circular formation of agents to the location of the source. The agents are stabilized to a circular formation by the cooperative formation control law explained in Section II. In order to implement both the formation control and the source seeking algorithm, the parameter  $\varepsilon$  must be chosen properly to guarantee the separation of time-scales, to ensure that the velocity of the centers  $c_i$  is bounded, and that the following condition  $\|\dot{c}_i(t)\| < D|\omega_0|, \forall i$  is satisfied; see [6].

As shown in Lemma 1, the gradient estimation accuracy depends on the formation radius. Consequently, we conclude that the radius  $D$  of the circular formation has a very important role in the stability of the algorithm, the speed of convergence, the noise attenuation and to determine the domain of convergence. In ongoing research, we seek the optimal value

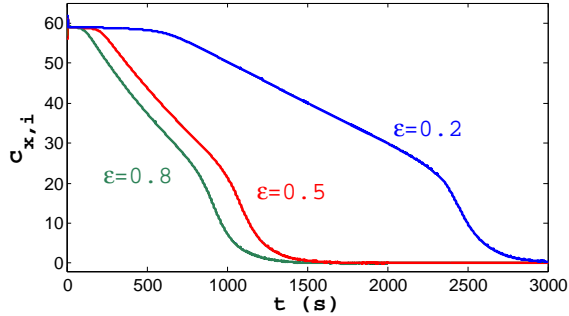


Fig. 3: Influence of parameter  $\varepsilon$  in the convergence rate of the proposed source seeking strategy.

of  $D$  that improves the convergence of our source seeking algorithm.

## V. SIMULATION RESULTS

In this section, we present some simulations to show the convergence of the proposed source seeking algorithm. For all simulations of sections V-A, V-B and V-C, the scalar field is a combination of two ellipses and thus with non-convex level curves given by

$$\sigma_1(z) = \exp(-z^T S_1 z) + \exp(-z^T R(\pi/4)^T S_2 R(\pi/4) z),$$

where  $S_1 = \frac{1}{100} \begin{bmatrix} 1/\sqrt{30} & 0 \\ 0 & 1 \end{bmatrix}$ ,  $S_2 = \frac{1}{100} \begin{bmatrix} 1 & 0 \\ 0 & 1/\sqrt{15} \end{bmatrix}$ . The maximum corresponding to the source is located at  $z_1^* = [0, 0]^T$  represented by the black  $\times$ . The communication topology is a ring, where agent  $i$  can communicate only to agents  $i-1$  and  $i+1$  modulo  $N$  neighbors, and thus the communication matrix is a symmetric circulant matrix given by

$$P = \begin{bmatrix} 1/2 & 1/4 & 0 & 1/4 \\ 1/4 & 1/2 & 1/4 & 0 \\ 0 & 1/4 & 1/2 & 1/4 \\ 1/4 & 0 & 1/4 & 1/2 \end{bmatrix}$$

In order to combine the circular formation control law in continuous time and the source seeking algorithm in discrete time, the first and second derivatives of the center trajectories,  $\dot{c}_i$  and  $\ddot{c}_i$ , are computed as discrete derivatives and filtered to obtain a smooth continuous signal.

### A. Source seeking without noise

Firstly, the case without noise is studied. Each agent measures the scalar field of interest at its position as  $\sigma(r_i)$ . Fig. 2 shows a simulation of four agents, whose dynamics are given by (1), computing the formation control law from Corollary 1 of our previous work [6] with radius  $D = 2$  and  $\omega_0 = 1$ . Algorithm 1 is then implemented in order to generate the centers' trajectories. The control parameters are  $\varepsilon = 0.5$  and  $\alpha = 1$ . The agents are displayed in green at three different instants: the initial conditions, an intermediate state at  $t = 500s$  and the final state at  $t = 2000s$ . The red lines represent the trajectories of centers  $c_i$  during the source seeking task. Thanks to Algorithm 1, the fleet of agents reaches a consensus on the center position and the formation is steered to the neighborhood of the source location.

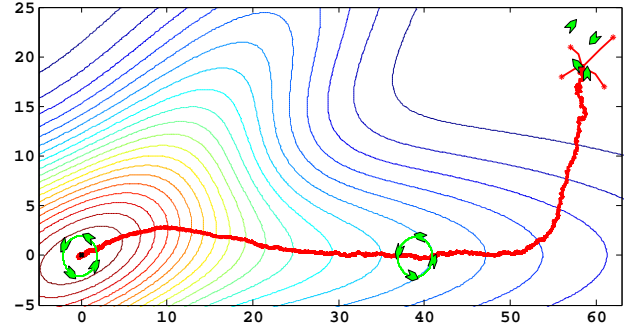


Fig. 4: Four agents collecting signal measurements corrupted by noise implement the proposed source seeking strategy ( $\varepsilon = 0.5$ ,  $\alpha = 0.5$ ).

In order to study the influence of the various parameters of Algorithm 1 on the convergence to the source location, several simulation results are shown in the sequel. Due to Theorem 1, with regard to ensure the separation of time-scales, the parameter  $\varepsilon$  must be chosen depending on the complexity of the scalar field and on the radius of the circular formation. Although the signal strength is unknown, we can always find a sufficiently small value of  $\varepsilon$  that satisfies the conditions of the theorem.

Fig. 3 displays the evolution of the first component of the centers' trajectories  $c_{x,i}(t)$  for three simulations of four agents implementing the proposed strategy with  $\alpha = 1$  and three values of  $\varepsilon$ . The convergence rate to reach the source position for each simulation with  $\varepsilon = 0.8$ ,  $\varepsilon = 0.5$  and  $\varepsilon = 0.2$  are, respectively,  $t = 1500s$ ,  $t = 1800s$ , and  $t = 3000s$ . Reasonably, the larger the value of  $\varepsilon$  the faster the convergence of the algorithm and the faster the circular formation reaches the source location.

### B. Source seeking with noisy measurements

We consider now that the signal measurements collected by each agent are corrupted by zero-mean Gaussian noise  $\omega_i(k) \sim \mathcal{N}(0, 0.2)$ . In this situation, the low-pass filter present in Algorithm 1 has an important role. Due to the noisy measurements, the error in the gradient estimate is greater than in the previous case without noise, and thus the centers  $c_i$  converge to a greater neighborhood of the source location  $z^*$ . Fig. 4 shows a simulation of four agents modeled by the unicycle dynamics (1) implementing the source seeking strategy. Algorithm 1 generates the centers' trajectories for the circular formation of agents with radius  $D = 2$  and  $\omega_0 = 1$ . The control parameters are  $\varepsilon = 0.5$  and  $\alpha = 0.5$ . The fleet of agents reaches a consensus on the center position and the formation is steered to the neighborhood of the source location.

The influence of the filter, regulated by the parameter  $\alpha$ , is also studied. Fig. 5 displays the evolution of the first component of the centers' trajectories,  $c_{x,i}$ , for three simulations of four agents computing Algorithm 1 with  $\varepsilon = 0.5$  and three values of  $\alpha$ . The signal measurements are corrupted by zero-mean Gaussian noise  $\omega_i(k) \sim \mathcal{N}(0, 0.2)$ . The convergence rate to reach the source position for each simulation with  $\alpha = 0.8$ ,



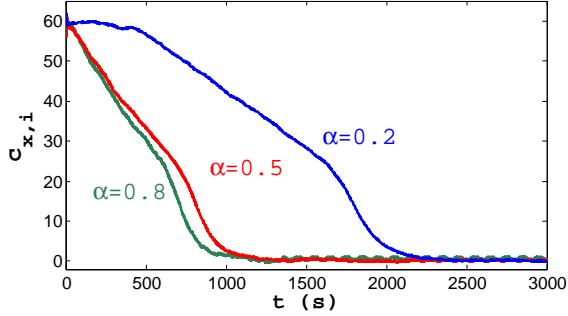


Fig. 5: Influence of parameter  $\alpha$  in the convergence rate of the proposed source seeking strategy.

$\alpha = 0.5$  and  $\alpha = 0.2$  is, respectively,  $t = 1500s$ ,  $t = 2000s$  and  $t = 3000s$ . The low-pass filter regulated by parameter  $\alpha$  allows attenuating the measurement noise and hence the centers' trajectories are *smoother* for smaller values of  $\alpha$ . However, the smaller this parameter is, the slower the convergence to the source location.

### C. Asynchronous communication

Here we analyze the case in which the communication between the agents is asynchronous. Following the ideas of [31], the new asynchronous communication matrix  $P(k)$  is built upon the standard symmetric gossip consensus. At every time step a single agent is activated, then this agent selects one of its neighbors and communicates with it; at each iteration  $k$  only two agents are able to exchange information. Therefore, the consensus of the quantities  $\tilde{h}_i(k)$  in Algorithm 1 is slower than in the synchronous situation. Consequently, the distributed source seeking algorithm requires smaller values of the parameter  $\varepsilon$ . Note that the asynchronous communication is only considered to implement Algorithm 1. However, to maintain the agents uniformly distributed along the formation, they still need to continuously receive information in a circulant communication topology.

Fig. 6 displays the evolution of the first component of the centers' trajectories,  $c_{x,i}(k)$ , in discrete-time for two simulations of four agents computing Algorithm 1 with  $\varepsilon = 0.2$ . In the first case, noise is not considered and  $\alpha = 1$  (red line). In the second case, the signal measurements are corrupted by zero-mean Gaussian noise  $\omega_i(k) \sim \mathcal{N}(0, 0.2)$  and  $\alpha = 0.5$  (blue line). These numerical results show that thanks to the inherent properties of the consensus protocols, our distributed source seeking algorithm also works in the case of asynchronous communication.

### D. Multiple or time-varying sources

To show the performance of our algorithm and also its limitations, a scenario with two sources is considered. Now, the scalar field is given by

$$\sigma_2(z) = \sigma_1(z) + \exp(-(z - z_2^*)^T R(3\pi/4)^T S_2 R(3\pi/4)(z - z_2^*)),$$

where  $S_2$  and  $\sigma_1(z)$  are as defined previously. As in the previous case, one source is located at the origin  $z_1^*$  and the

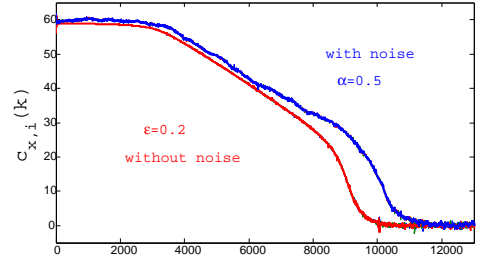


Fig. 6: Source seeking Algorithm 1 with asynchronous communication for two simulations without and with noisy measurements.

second one is located at  $z_2^* = [30, 30]^T$ , both represented by black  $\times$ . The communication topology considered is a ring.

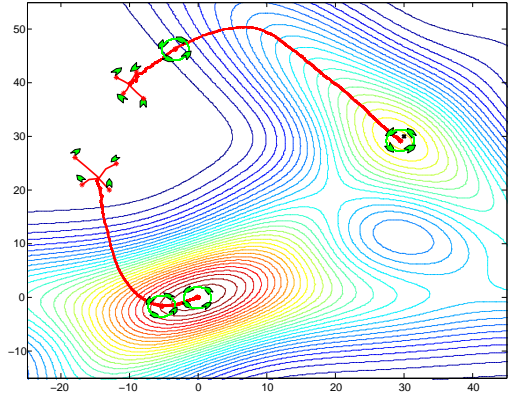


Fig. 7: Two simulations of four agents collecting noisy measurements implementing the proposed source seeking strategy starting from different initial conditions.

Fig. 7 displays two different simulations of four unicycle-like agents implementing the circular formation control law from [6] with  $D = 2$  and  $\omega_0 = 1$  and computing Algorithm 1 to generate the centers' trajectories with  $\varepsilon = 0.5$  and  $\alpha = 0.5$ . The agents are displayed in green at three different instants, initial conditions,  $t = 250s$  and  $t = 3000s$ . For each simulation, the initial conditions are different in order to show the local stability properties of our approach. In the case of multiple sources, the agents converge to a local maximum depending on their initial conditions. As shown in Fig. 7, the convergence rate depends also on the initial conditions and the shape of the signal measured.

Fig. 8 show a simulation of four agents in a time-varying environment. The simulation starts in the same scenario as in Fig. 7 and the agents converge to a local maximum located in the neighborhood of the second source  $z_2^*$ . At instant  $t = 2000s$  the scalar field  $\sigma_2(z)$  vanishes and then the formation of agents driven by Algorithm 1 travels towards the source of  $\sigma_1$  located at the origin. At instant  $t = 3000s$  this source also vanishes and therefore there is no field to be measured and the center of the formation moves following a random walk due to the noisy measurements. The initial scalar field  $\sigma_2$  is displayed in gray.

The quadratic case has been also studied through numerical

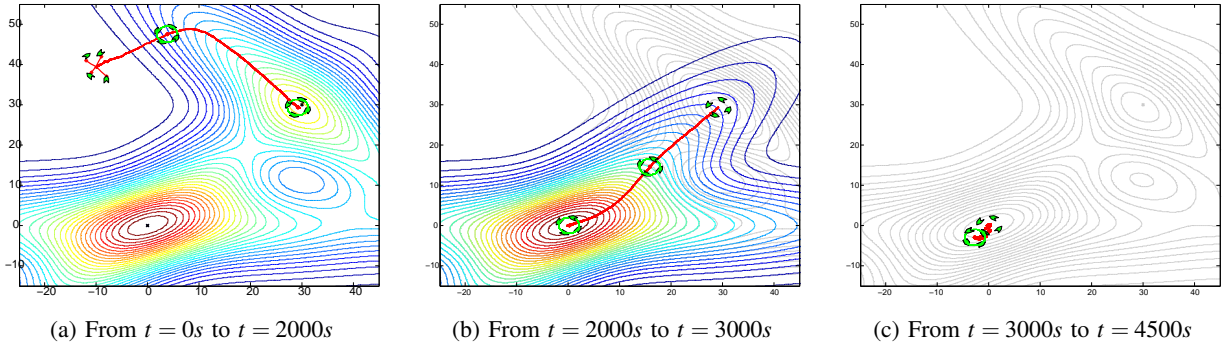


Fig. 8: Simulation of four agents computing the proposed distributed source seeking strategy in a time-varying environment.

simulations concluding that the behavior and convergence rate is the same that using a standard gradient-ascent algorithm. Videos showing more simulations are accessible online<sup>1</sup>.

## VI. CONCLUSION AND FUTURE WORK

This paper provides a distributed solution to the 2-dimensional source localization problem. Our cooperative approach considers a group of unicycle-like agents, which are able to measure the signal distribution emitted by the source. Firstly, thanks to the circular formation control from our previous work [6], the nonlinear vehicles can be stabilized to a time-varying circular formation. Then, we have shown that collecting the measurements of the agents uniformly distributed along the formation, the gradient of the signal strength at the center can be estimated. Using this information, a distributed source seeking algorithm is proposed to provide the trajectory of the center in order to steer the fleet of vehicles to the source location. This result is based on consensus algorithms and thus can deal with several communication constraints and can be applied also in the case of asynchronous communication. Our solution allows maintaining the circular formation, estimating the gradient of the signal and driving the center of the formation to the maximum of the scalar field of interest. Moreover, we include a low-pass filter in order to make the algorithm more robust to measurement noise.

Future work will be focused on extending this approach to the 3-dimensional case. Another future direction is to approximate the Hessian of the signal distribution at the center of the circular formation in order to improve the convergence rate of our source seeking algorithm. In addition, to improve our distributed algorithm and its convergence properties, the control of the radius of the formation will be a key point in future research.

## APPENDIX

### Proof of Theorem 1:

Introducing the additional variable  $\mathbf{v}(k) = \mathbf{g}(k-1)$  where  $\mathbf{g}(k) = [g_1(k)^T, \dots, g_N(k)^T]^T \in \mathbb{R}^{2N}$ , Algorithm 1 can be rewritten as

$$\begin{aligned} \mathbf{v}(k) &= \mathbf{g}(k-1) \\ \mathbf{h}(k) &= (\mathbf{P} \otimes \mathbf{I}_2)(\mathbf{h}(k-1) + \mathbf{g}(k-1) - \mathbf{v}(k-1)) \\ c_i(k) &= (1 - \varepsilon)c_i(k-1) + \varepsilon h_i(k). \end{aligned} \quad (9)$$

This system is the Euler discretization with time interval  $T = \varepsilon$  of the following continuous-time system

$$\begin{aligned} \varepsilon \dot{\mathbf{v}}(t) &= -\mathbf{v}(t) + \mathbf{g}(t) \\ \varepsilon \dot{\mathbf{h}}(t) &= -\mathbf{K}\mathbf{h}(t) + (\mathbf{I}_{2N} - \mathbf{K})(\mathbf{g}(t) - \mathbf{v}(t)) \\ \dot{c}_i(t) &= -c_i(t) + h_i(t), \end{aligned} \quad (10)$$

where  $\mathbf{K} = \mathbf{I}_{2N} - (\mathbf{P} \otimes \mathbf{I}_2)$ . If the parameter  $\varepsilon$  is sufficiently small, the discretized system (9) inherits the stability properties of system (10). This system is composed by two different time-scale subsystems regulated by the parameter  $\varepsilon$ . The convergence properties can be proved by exploiting Theorem 11.4 from [12]. The idea is to analyze separately the convergence of the reduced system (slow dynamics) and the boundary layer system (fast dynamics).

Firstly, we define the change of variables  $\mathbf{d}(t) = \mathbf{h}(t) - \mathbf{v}(t)$ , which implies

$$\varepsilon(\dot{\mathbf{d}}(t) + \dot{\mathbf{v}}(t)) = -\mathbf{K}(\mathbf{d}(t) + \mathbf{v}(t)) + (\mathbf{I}_{2N} - \mathbf{K})(\mathbf{g}(t) - \mathbf{v}(t))$$

and, due to the dynamics (10), then

$$\varepsilon \dot{\mathbf{d}}(t) = -\mathbf{K}(\mathbf{d}(t) - \mathbf{g}(t)). \quad (11)$$

In order to decompose Eq. (11) in two projections we use the following definitions:

$$\mathbf{\Pi}^{\parallel} = \frac{\mathbf{I}_N \mathbf{I}_N^T}{N} \otimes \mathbf{I}_2 \quad \text{and} \quad \mathbf{\Pi}^{\perp} = \left( \mathbf{I}_N - \frac{\mathbf{I}_N \mathbf{I}_N^T}{N} \right) \otimes \mathbf{I}_2.$$

Moreover,  $\mathbf{c}^{\parallel} = \mathbf{\Pi}^{\parallel} \mathbf{c}(k)$  and  $\mathbf{c}^{\perp} = \mathbf{\Pi}^{\perp} \mathbf{c}(k)$ . By definition,  $\mathbf{\Pi}^{\parallel} \mathbf{K} = 0$  and  $\mathbf{\Pi}^{\perp} \mathbf{K} = \mathbf{K}$ . Defining the decomposition  $\mathbf{d}(t) = \mathbf{d}^{\parallel} + \mathbf{d}^{\perp}$ , Eq. (11) can be also decomposed as

$$\varepsilon \dot{\mathbf{d}}^{\parallel}(t) = 0 \quad \text{and} \quad \varepsilon \dot{\mathbf{d}}^{\perp}(t) = -\mathbf{K}(\mathbf{d}^{\perp}(t) + \mathbf{g}(t)).$$

Then, system (10) becomes

$$\begin{aligned} \varepsilon \dot{\mathbf{v}}(t) &= -\mathbf{v}(t) + \mathbf{g}(t) \\ \varepsilon \dot{\mathbf{d}}^{\perp}(t) &= -\mathbf{K}(\mathbf{d}^{\perp}(t) + \mathbf{g}(t)) \\ \dot{c}_i(t) &= -c_i(t) + [\mathbf{d}^{\perp}(t) + \mathbf{v}(t)]_i \end{aligned} \quad (12)$$

where  $[\cdot]_i$  denotes the submatrix of the operand that is relative to agent  $i$ .

Following the singular perturbation model analysis we study both slow and fast dynamics of system (10). To analyze the behavior of the boundary layer system assume that  $c_i(t) = c_i \forall i$  and thus we can write  $\mathbf{c}(t) = \mathbf{c}$  and  $\mathbf{g}(t) = \mathbf{g}(\mathbf{c})$  with  $\mathbf{c}$  constant in time. Consider the system

<sup>1</sup>Simulations are accessible in <https://sites.google.com/site/lbrinonarranz/videos>

$$\begin{aligned}\varepsilon \dot{\mathbf{v}}(t) &= -\mathbf{v}(t) + \mathbf{g}(\mathbf{c}) \\ \varepsilon \dot{\mathbf{d}}^\perp(t) &= -K(\mathbf{d}^\perp(t) + \mathbf{g}(\mathbf{c})).\end{aligned}\quad (13)$$

Applying the change of variables induced by the isolated root of (13), namely,

$$\tilde{\mathbf{v}}(t) = \mathbf{v}(t) - \mathbf{g}(\mathbf{c}), \quad \tilde{\mathbf{d}}^\perp(t) = -K(\mathbf{d}^\perp(t) - \mathbf{g}^\perp(\mathbf{c})), \quad \tau = \frac{t}{\varepsilon},$$

an exponentially stable boundary-layer system is obtained, i.e.,

$$\begin{aligned}\dot{\tilde{\mathbf{v}}}(\tau) &= -\tilde{\mathbf{v}}(\tau) \\ \dot{\tilde{\mathbf{d}}}^\perp(\tau) &= -K\tilde{\mathbf{d}}^\perp(\tau).\end{aligned}\quad (14)$$

Therefore

$$\lim_{t \rightarrow \infty} \begin{pmatrix} \mathbf{v}(t) \\ \mathbf{d}^\perp(t) \end{pmatrix} = \begin{pmatrix} \mathbf{g}(\mathbf{c}) \\ -\mathbf{g}^\perp(\mathbf{c}) \end{pmatrix}.$$

To prove this property for the last equation consider for example the Lyapunov function  $V(\tilde{\mathbf{d}}^\perp) = \frac{1}{2}\|\tilde{\mathbf{d}}^\perp\|^2$  and its derivative  $\dot{V}(\tilde{\mathbf{d}}^\perp) = -(\tilde{\mathbf{d}}^\perp)^T K \tilde{\mathbf{d}}^\perp \leq -\lambda_2 \|\tilde{\mathbf{d}}^\perp\|^2 \leq -\lambda_2 V(\tilde{\mathbf{d}}^\perp)$ , where  $\lambda_2$  denotes the smallest non-zero eigenvalue of matrix  $K$ . Therefore,  $\tilde{\mathbf{d}}^\perp$  converges to zero exponentially.

Given the analysis of the boundary layer system above, if we substitute the previous equilibrium points into the last equation of system (12) we obtain the reduced system

$$\dot{c}_i(t) = -c_i(t) + [\mathbf{g}^\parallel(\mathbf{c}(t))]_i, \quad (15)$$

where

$$\begin{aligned}\mathbf{g}^\parallel(\mathbf{c}(t)) &= \left[ \frac{1}{N} \sum_{i=1}^N \left( c_i(t) + \frac{2}{D^2} \sigma(r_i(t))(r_i(t) - c_i(t)) \right) \right] \otimes \mathbf{I}_N \\ &= \bar{\mathbf{g}}(\mathbf{c}(t)) \otimes \mathbf{I}_N\end{aligned}$$

and we get

$$\dot{c}_i(t) = -c_i(t) + \bar{g}(\mathbf{c}(t)). \quad (16)$$

We rewrite Eq. 16 in a compact way

$$\dot{\mathbf{c}}(t) = -\mathbf{c}(t) + \bar{\mathbf{g}}(\mathbf{c}(t)) \otimes \mathbf{I}_N$$

and decomposing it along the projections  $\Pi^\parallel$  and  $\Pi^\perp$

$$\dot{\mathbf{c}}^\parallel(t) = -\mathbf{c}^\parallel(t) + \bar{\mathbf{g}}(\mathbf{c}^\parallel(t) + \mathbf{c}^\perp(t)) \otimes \mathbf{I}_N \quad \text{and} \quad \dot{\mathbf{c}}^\perp(t) = -\mathbf{c}^\perp(t)$$

since  $\Pi^\perp(A \otimes \mathbf{I}_N) = \mathbf{0}$  for all  $A \in \mathbb{R}^{2 \times 2}$ . Since the dynamics of  $\mathbf{c}^\perp(t)$  are exponentially stable,  $\mathbf{c}^\perp(t)$  is bounded. Considering  $\mathbf{c}^\parallel(t) = \bar{\mathbf{c}}(t) \otimes \mathbf{I}_N$ , we can restrict our attention to the dynamics of the average, i.e.,

$$\dot{\bar{\mathbf{c}}}(t) = -\bar{\mathbf{c}}(t) + \bar{\mathbf{g}}(\bar{\mathbf{c}}(t) + \mathbf{c}^\perp(t)).$$

Using (2) to express the position of the agents, we have the following result

$$\begin{aligned}\bar{\mathbf{g}}(\mathbf{c}(t)) &= \bar{\mathbf{c}}(t) + \frac{2}{ND^2} \sum_{i=1}^N \sigma(r_i(t))(r_i(t) - c_i(t)) \\ &= \frac{2}{ND^2} \sum_{i=1}^N \sigma(\bar{\mathbf{c}}(t) + c_i^\perp(t) + e_i(t))e_i(t) \\ &= \frac{2}{ND^2} \sum_{i=1}^N \sigma(\bar{\mathbf{c}} + e_i)e_i \\ &+ \frac{2}{ND^2} \sum_{i=1}^N [\sigma(\bar{\mathbf{c}} + c_i^\perp + e_i) - \sigma(\bar{\mathbf{c}} + e_i)] e_i \\ &= \frac{2}{ND^2} \sum_{i=1}^N \sigma(\bar{\mathbf{c}} + e_i)e_i + \Psi(D, \mathbf{c}).\end{aligned}$$

According to Lemma 1 the dynamics of  $\bar{\mathbf{c}}$  are given by

$$\dot{\bar{\mathbf{c}}}(t) = \nabla \sigma(\bar{\mathbf{c}}) + \varphi(D, \bar{\mathbf{c}}) + \Psi(D, \mathbf{c}), \quad (17)$$

which is the standard gradient ascent algorithm apart from the approximation error  $\varphi(D, \bar{\mathbf{c}})$  and the perturbed term  $\Psi(D, \mathbf{c})$ .

The stability of the reduced system is analyzed using the Lyapunov function

$$V(\bar{\mathbf{c}}) = \sigma(\mathbf{z}^*) - \sigma(\bar{\mathbf{c}}) \geq 0,$$

which is positive definite since  $\mathbf{z}^*$  is the only minimum of the signal distribution. Differentiating along the solutions of (17), the following equation holds:

$$\begin{aligned}\dot{V}(\bar{\mathbf{c}}) &= -\|\nabla \sigma(\bar{\mathbf{c}})\|^2 - \nabla \sigma(\bar{\mathbf{c}})^T (\varphi(D, \bar{\mathbf{c}}) + \Psi(D, \mathbf{c})) \\ &\leq -\|\nabla \sigma(\bar{\mathbf{c}})\|^2 + \|\nabla \sigma(\bar{\mathbf{c}})\| (\|\varphi(D, \bar{\mathbf{c}})\| + \|\Psi(D, \mathbf{c})\|).\end{aligned}$$

Consider Assumption 1 and the Lipschitz constant  $L$ , then

$$\begin{aligned}\|\Psi(D, \mathbf{c})\| &\leq \frac{2}{ND^2} \sum_{i=1}^N \|\sigma(\bar{\mathbf{c}} + c_i^\perp + e_i) - \sigma(\bar{\mathbf{c}} + e_i)\| \|e_i\| \\ &\leq \frac{2L}{ND} \sum_{i=1}^N \|c_i^\perp(t)\|.\end{aligned}$$

Since  $\mathbf{c}^\perp(t)$  is bounded, we assume that  $\|c_i^\perp(t)\| \leq \delta, \forall i$  and, using Lemma 1, we know that  $\|\varphi(D, \bar{\mathbf{c}})\| \leq \lambda_{\max}(H_\sigma)D$ . The following inequality is obtained:

$$\begin{aligned}\dot{V}(\bar{\mathbf{c}}) &\leq -\|\nabla \sigma(\bar{\mathbf{c}})\|^2 + \|\nabla \sigma(\bar{\mathbf{c}})\| (\lambda_{\max}(H_\sigma)D + \frac{2L}{D}\delta) \\ &\leq -\|\nabla \sigma(\bar{\mathbf{c}})\| (\|\nabla \sigma(\bar{\mathbf{c}})\| - \lambda_{\max}(H_\sigma)D - \frac{2L}{D}\delta).\end{aligned}$$

Therefore,  $\dot{V}(\bar{\mathbf{c}}) \leq 0$  when  $\|\nabla \sigma(\bar{\mathbf{c}})\| \geq \lambda_{\max}(H_\sigma)D + \frac{2L}{D}\delta = \beta$ . Considering Assumption 1,  $\dot{V}(\bar{\mathbf{c}}) \leq 0$  when  $\|\bar{\mathbf{c}}\| \geq \frac{1}{a_3}(\lambda_{\max}(H_\sigma)D + \frac{2L}{D}\delta)$ . Let  $\Omega_l = \{\bar{\mathbf{c}} : \|\bar{\mathbf{c}}\| \leq l\} = \beta$  be a level set of the Lyapunov function  $V(\bar{\mathbf{c}})$  with  $l = a_2\beta^2$ . Without loss of generality, we assume that the minimum of the signal strength corresponds to the origin, s.t.,  $\mathbf{z}^* = \mathbf{0}$ . Then, the closed ball  $B_\beta$  centered at  $\bar{\mathbf{c}} = \mathbf{0}$  and with radius  $\beta$  is contained in  $\Omega_l$  because

$$\|\bar{\mathbf{c}}\| \leq \beta \Rightarrow V(\bar{\mathbf{c}}) \leq a_2\|\bar{\mathbf{c}}\|^2 \leq a_2\beta^2 = l,$$

and thus  $\bar{\mathbf{c}} \in \Omega_l$ . As a result, any solution of (17) starting in  $\mathbb{R}^2/\Omega_l$  satisfies  $\dot{V}(\bar{\mathbf{c}}) < 0$ . Thus, it enters  $\Omega_l$  in finite time and remains in  $\Omega_l$  thereafter. This guarantees asymptotic stability of  $\bar{\mathbf{c}} = \mathbf{0}$  with a radius  $\gamma(D, H_\sigma, \delta)$ . To obtain the value of  $\gamma$  we use the lower bound of the signal distribution according to Assumption 1, such that

$$a_1\|\bar{\mathbf{c}}\|^2 \leq V(\bar{\mathbf{c}}) \leq a_2\beta^2$$

and thus the solutions enter the region  $\|\bar{\mathbf{c}}\| \leq \beta \sqrt{\frac{a_2}{a_1}}$ . This implies that the radius of the  $\gamma$ -stability is

$$\gamma = \frac{1}{a_3} \left( \lambda_{\max}(H_\sigma)D + \frac{2L}{D}\delta \right) \sqrt{\frac{a_2}{a_1}}.$$

The  $\gamma$ -stability of  $\bar{\mathbf{c}}(t) = \mathbf{z}^*$  implies that  $\|\bar{\mathbf{c}}(t) - \mathbf{z}^*\| \leq \gamma$  as  $t \rightarrow \infty$ . If  $\varepsilon$  is sufficiently small then, the separation of time scales holds and  $\lim_{k \rightarrow \infty} c_i(k) = \lim_{k \rightarrow \infty} \bar{\mathbf{c}}(k)$ , which converges asymptotically to the neighborhood of the minimum of the signal strength. Note that, in the quadratic case, the approximation term  $\varphi(D, \mathbf{c})$  vanishes because by Lemma 1 we obtain  $\dot{\bar{\mathbf{c}}}(t) = -\nabla \sigma(\bar{\mathbf{c}}) + \Psi(D, \mathbf{c})$  and, the radius of the  $\gamma$ -stability is reduced to

$$\gamma = \frac{2L\delta}{a_3D} \sqrt{\frac{a_2}{a_1}}.$$

## REFERENCES

- [1] S. Azuma, M. S. Sakar, and G. J. Pappas. Stochastic source seeking by mobile robots. *IEEE Trans. Autom. Control*, 57:2308–2321, 2012.
- [2] R. Bachmayer and N. E. Leonard. Vehicle networks for gradient descent in a sampled environment. In *Proc. of the 41st IEEE Conference on Decision and Control*, pages 112–117, 2002.
- [3] E. Biyik and M. Arcak. Gradient climbing in formation via extremum seeking and passivity-based coordination rules. *Asian Journal of Control, Special Issue on Collective Behavior and Control of Multi-Agent Systems*, 10(2):201–211, 2008.
- [4] L. Briñón-Arranz and L. Schenato. Consensus-based source-seeking with a circular formation of agents. In *Proc. of the 2013 European Control Conference*, 2013.

- [5] L. Briñón-Arranz, A. Seuret, and C. Canudas-de-Wit. Collaborative estimation of gradient direction by a formation of AUVs under communication constraints. In *Proc. of the 50th IEEE Conference on Decision and Control*, pages 5583–5588, 2011.
- [6] L. Briñón-Arranz, A. Seuret, and C. Canudas-de-Wit. Cooperative control design for time-varying formations of multi-agent systems. *IEEE Trans. Autom. Control*, 59(8):2283–2288, 2014.
- [7] J. Choi, S. Oh, and R. Horowitz. Distributed learning and cooperative control for multi-agent systems. *Automatica*, 45:2802–2814, 2009.
- [8] J. Cochran and M. Krstić. Nonholonomic source seeking with tuning of angular velocity. *IEEE Trans. Autom. Control*, 54(4):717–731, 2009.
- [9] E. Fiorelli, P. Bhatta, N. E. Leonard, and I. Shulman. Adaptive sampling using feedback control of an autonomous underwater glider fleet. In *Proc. of 13th Inter. Symposium on Unmanned Untethered Submersible Technology*, pages 1–16, 2003.
- [10] F. Garin and L. Schenato. *Networked Control Systems, ch. A survey on distributed estimation and control applications using linear consensus algorithms*. Springer, 2011.
- [11] M. Jadhaliha, J. Lee, and J. Choi. Adaptive control of multi-agent systems for finding peaks of uncertain static fields. *Journal of Dynamic Systems, Measurements and Control*, 134(5), 2012.
- [12] H. Khalil. *Nonlinear Systems*. Prentice Hall, third edition 2002.
- [13] S. Z. Khong, Y. Tan, C. Manzie, and D. Nesić. Multi-agent source seeking via discrete-time extremum seeking control. *Automatica*, 50:2312–2320, 2014.
- [14] V. Kumar, D. Rus, and S. Singh. Robot and sensor networks for first responders. *IEEE Pervasive Computing*, 3:24–33, 2004.
- [15] S. Li and Y. Guo. Distributed source seeking by cooperative robots: All-to-all and limited communications. In *Proc. of the 2012 IEEE Inter. Conference on Robotics and Automation*, pages 1107–1112, 2012.
- [16] S. Li, R. Kong, and Y. Guo. Cooperative distributed source seeking by multiple robots: Algorithms and experiments. *IEEE Trans. Mechatronics*, 19:1810–1820, 2014.
- [17] W. Li, J. Farrell, S. Pang, and R. Arrieta. Moth-inspired chemical plume tracing on an autonomous underwater vehicle. *IEEE Trans. Robotics*, 22:292–307, 2006.
- [18] S.-J. Liu and M. Krstić. Stochastic source seeking for nonholonomic unicycle. *Automatica*, 46:1443–1453, 2010.
- [19] L. Marques, U. Nunes, and A. de Almeida. Particle swarm-based olfactory guided search. *Autonomous Robots*, 20:277–287, 2006.
- [20] A. S. Matveev, M. C. Hoy, and A. V. Savkin. Reactive navigation of a mobile robot to the moving extremum of a dynamic unknown environmental field without derivative estimation. In *Proc. of the 2013 European Control Conference*, 2013.
- [21] A. R. Mesquita, J. P. Hespanha, and K. Astrom. Optimotaxis: a stochastic multi-agent optimization procedure with point measurements. *Lecture Notes in Computer Science*, 4981:358–371, 2008.
- [22] B. J. Moore and C. Canudas-de-Wit. Source seeking via collaborative measurements by a circular formation of agents. In *Proc. of the 2010 IEEE American Control Conference*, pages 6417–6422, 2010.
- [23] P. Ogren, E. Fiorelli, and N. E. Leonard. Cooperative control of mobile sensor networks: Adaptive gradient climbing in a distributed environment. *IEEE Trans. Autom. Control*, 49:1292–1302, 2004.
- [24] M. Rabbat and R. Nowak. Distributed optimization in sensor networks. In *Proc. of the 3rd Inter. Symposium on Information Processing in Sensor Networks*, pages 20–27, 2004.
- [25] S. S. Sahyoun, S. M. Djouadi, and H. Qi. Dynamic plume tracking using mobile sensors. In *Proc. of the 2010 American Control Conference*, pages 2915–2920, 2010.
- [26] M. S. Stanković and D. M. Stipanović. Extremum seeking under stochastic noise and applications to mobile sensors. *Automatica*, 46:1243–1251, 2010.
- [27] V. Rigaud, J. L. Michel et al. First steps in Ifremer’s autonomous underwater vehicle program—a 3000m depth operational survey AUV for environmental monitoring. In *Proc. of the 14th Intern. Offshore and Polar Engineering Conference*, 2004.
- [28] W. Wu, I. D. Couzin, and F. Zhang. Bio-inspired source seeking with no explicit gradient estimation. In *3rd IFAC Workshop on Distributed Estimation and Control in Networked Systems*, pages 240–245, 2012.
- [29] W. Wu and F. Zhang. Cooperative exploration of level surfaces of three dimensional scalar fields. *Automatica*, 47(9):2044–2051, 2011.
- [30] W. Wu and F. Zhang. Robust cooperative exploration with a switching strategy. *IEEE Trans. Robotics*, 28(4):828–839, 2012.
- [31] F. Zanella, D. Varagnolo, A. Cenedese, G. Pillonetto, and L. Schenato. Asynchronous newton-raphson consensus for distributed convex optimization. In *3rd IFAC Workshop on Distributed Estimation and Control in Networked Systems*, 2012.
- [32] F. Zanella, D. Varagnolo, A. Cenedese, G. Pillonetto, and L. Schenato. Multidimensional Newton-Raphson consensus for distributed convex optimization. In *Proc. of the 2012 American Control Conference*, pages 1079–1084, 2012.
- [33] C. Zhang, D. Arnold, N. Ghods, A. Siranosian, and M. Krstić. Source seeking with non-holonomic unicycle without position measurement and with tuning of forward velocity. *Systems & Control Letters*, 56:245–252, 2007.
- [34] C. Zhang, D. Florencio, D. E. Ba, and Z. Zhang. Maximum likelihood sound source localization and beamforming for directional microphone arrays in distributed meetings. *IEEE Trans. Multimedia*, 10:538–548, 2008.
- [35] F. Zhang and N. E. Leonard. Cooperative filters and control for cooperative exploration. *IEEE Trans. Autom. Control*, 55:650–663, 2010.
- [36] S. Zhu, D. Wang, and C. B. Low. Cooperative control of multiple UAVs for source seeking. *Journal of Intelligent and Robotic Systems*, 70:293–301, 2013.



**Lara Briñón-Arranz** received the M.S. degree in Automation and Electronics Engineering from the Technical University of Madrid, Spain, and the M.S. degree in Control Engineering from the Grenoble Institute of Technology (Grenoble-INP), France, in 2008. She received the Ph.D. degree in Control Engineering from the University of Grenoble in 2011. She held a postdoctoral position at the Grenoble-INP in 2011-2012. From 2013 to 2014 she was postdoctoral scholar at the Instituto Superior Técnico, Lisbon, Portugal. Currently she is a researcher engineering at the Laboratory for Analysis and Architecture of Systems (LAAS), Toulouse, France. Her interests include cooperative control, networked control systems, distributed estimation and multi-agent systems.



**Luca Schenato** (M’07) received the Dr. Eng. degree in Electrical Engineering from the University of Padova in 1999 and the Ph.D. degree in Electrical Engineering and Computer Sciences from the UC Berkeley, in 2003. He held a post-doctoral position in 2004 and a visiting professor position in 2013-2014 at U.C. Berkeley. Currently he is Associate Professor at the Information Engineering Department at the University of Padova. His interests include networked control systems, multi-agent systems, wireless sensor networks, smart grids and cooperative robotics.

Prof. Schenato has been awarded the 2004 Researchers Mobility Fellowship by the Italian Ministry of Education, University and Research (MIUR), and the 2006 Eli Jury Award in U.C. Berkeley and the EUCA European Control Award in 2014. He served as Associate Editor for *IEEE Trans. Autom. Control* from 2010 to 2014.



**Alexandre Seuret** earned the Engineer’s degree from the Ecole Centrale de Lille, France and the M.S. degree from the University of Science and Technology of Lille in 2003. He received the Ph.D. degree in Automatic Control from the Ecole Centrale de Lille and the University of Science and Technology of Lille in 2006. From 2006 to 2008, he held one-year postdoctoral positions at the University of Leicester, UK and the Royal Institute of Technology (KTH), Stockholm, Sweden. From 2008 to 2012, he was a junior CNRS researcher (Chargé de Recherche) at the GIPSA-Lab in Grenoble, France. Since 2012, he has been with the Laboratory for Analysis and Architecture of Systems (LAAS), Toulouse, France. His research interests include time-delay systems, networked control systems and multi-agent systems.